



OPEN

A critical re-evaluation of the slope factor of the operational model of agonism: When to exponentiate operational efficacy

Alena Randáková, Dominik Nelic & Jan Jakubík

Agonist efficacy denoting the “strength” of agonist action is a cornerstone in the proper assessment of agonist selectivity and signalling bias. The simulation models are very accurate but complex and hard to fit experimental data. The parsimonious operational model of agonism (OMA) has become successful in the determination of agonist efficacies and ranking them. In 1983, Black and Leff introduced the slope factor to the OMA to make it more flexible and allow for fitting steep as well as flat concentration–response curves. First, we performed a functional analysis to indicate the potential pitfalls of the OMA. Namely, exponentiation of operational efficacy may break relationships among the OMA parameters. The fitting of the Black & Leff equation to the theoretical curves of several models of functional responses and the experimental data confirmed the fickleness of the exponentiation of operational efficacy affecting estimates of operational efficacy as well as other OMA parameters. In contrast, fitting The OMA based on the Hill equation to the same data led to better estimates of model parameters. In conclusion, Hill equation-based OMA should be preferred over the Black & Leff equation when functional-response curves differ in the slope factor. Otherwise, the Black & Leff equation should be used with extreme caution acknowledging potential pitfalls.

In pharmacology, efficacy serves as a measure of how much response each ligand-receptor complex can produce upon its formation¹. A sound method to assess agonist efficacy is essential for research and drug discovery. The operational model of agonism (OMA) introduces the term operational efficacy². OMA has become a golden standard in the evaluation of agonism and subsequently also of signalling bias^{3–5}. The OMA describes the response of the system as a function of ligand concentration using three parameters: (1) The equilibrium dissociation constant of agonist (K_A) to the receptor initiating functional response; (2) The maximal possible response of the system (E_{MAX}); (3) The operational efficacy of agonist (τ). As we will show, in the OMA, K_A represents the affinity of the agonist for the receptor. Therefore, K_A is specific to a given combination of ligand and receptor. The maximal possible response of the system E_{MAX} is specific to the system. The operational efficacy (τ) is a measure of the response to a given agonist at a given system, ranging from 0 to infinity, and is specific to a combination of ligand and system.

OMA has numerous limitations and possible pitfalls. All three parameters (E_{MAX} , K_A , and τ) are inter-dependent, thus, one of them has to be predetermined before fitting OMA to data or the global fit of multiple curves at various receptor densities has to be performed⁶. Besides that, there are additional methodological and conceptual issues^{7–9}. Here we focus on the exponentiation of operational efficacy. In practice, positive cooperativity or positive feedback leads to steep and negative cooperativity or negative feedback leads to flat concentration–response curves that the OMA (Eq. (2)) does not fit. Therefore, an equation intended for the description of non-hyperbolic concentration curves (Eq. (7)) was introduced by Black et al.¹⁰. Since then, Eq. (7) has been commonly used. The presented simple mathematical analysis of Eq. (7) shows that the slope factor affects the relationship between observed maximal response to agonist (E'_{MAX}) and operational efficacy (τ) and the relationship between the concentration of agonist for half-maximal response (EC_{50}) and its equilibrium dissociation constant (K_A). Some combinations of operational efficacy and slope factor in the Black & Leff equation (Eq. (7)) lead to EC_{50} greater than K_A which is biochemically counterintuitive. In the system with receptor reserve maximum effect is reached before the occupation of all receptors is reached. Therefore, half of the effect (EC_{50}) is reached before reaching the occupation of half of all receptors (K_A). In a system without receptor reserve, full occupation of receptors

Institute of Physiology Czech Academy of Sciences, Vídeňská 1083, 142 20 Praha, Prague, Czech Republic. email: jan.jakubik@fgu.cas.cz

is reached before reaching system E_{MAX} . Therefore, EC_{50} occurs at K_A . Black & Leff model, however, allows for $EC_{50} > K_A$ in the systems with low efficacy and high slope factor.

The Hill equation was originally formulated to describe the binding of oxygen molecules to haemoglobin^{11,12}. The Hill equation was then incorporated into the first model of receptor function, the so-called occupation theory¹³. In contrast to the Black et al. slope factor, the slope factor of the Hill equation (Eq. (10)) does not affect the centre or asymptotes of the hyperbola describing concentration–response curves. Therefore, the Hill coefficient does not affect relationships between E'_{MAX} and τ nor between EC_{50} and K_A . This makes Hill equation-based OMA (Eq. (11)) more practical in many ways. Fitting the Black & Leff equation (Eq. (7)) to the theoretical data revealed several drawbacks, like under- or over-estimation of parameters or high levels of uncertainty of parameter estimates. Moreover, in contrast to Hill equation-based OMA (Eq. (11)), in some cases, fitting the Black & Leff equation to the experimental data resulted in the wrong ranking of agonist efficacies τ and wrong estimates of agonist K_A . However, it should be noted that the Black & Leff equation should not be used firsthandily as slopes of individual response curves vary among agonists.

The general concept of the operational model of agonism

For demonstrative purposes, we will derive OMA from scratch for receptor-effector systems. This will become handy for the analysis of systems with low expression of receptors. The OMA equation for ligand-gated ion channels is the same, although, it is based on different sets of equations. In general, OMA consists of two functions. One function describes the binding of an agonist to a receptor as the dependence of the concentration of agonist-receptor complexes [RA] on the concentration of an agonist [A]. The second function describes the dependence of functional response (E) on the concentration of agonist-receptor complexes [RA]. OMA expresses the dependence of response E on the concentration of [A].

Rectangular hyperbolic OMA

Definition of OMA

In the simplest case, when both binding and response functions are described by rectangular hyperbola (Supplementary Information Figure S1), the resulting function is also a rectangular hyperbola. For example, in a bimolecular reaction, the dependence of ligand binding to the receptor [RA] is described by Eq. (1) where [A] is the concentration of ligand and K_A is its equilibrium dissociation constant that represents the concentration of ligand at which half of the total number of receptors, R_T , binds the ligand and the other half of the receptors is free.

$$[RA] = \frac{R_T[A]}{[A] + K_A} \quad (1)$$

If the bound ligand is an agonist, it activates the receptor and produces functional response E. Response as a function of agonist binding (agonist-receptor complexes [RA]) is given by Eq. (2).

$$E = \frac{E_{MAX}[RA]}{[RA] + K_E} \quad (2)$$

where E_{MAX} is the maximum possible response of the system and K_E is the value of [RA] that elicits a half-maximal effect. Various agonists produce a functional response of different strengths. The OMA was postulated to introduce the “transducer ratio” τ that is given by Eq. (3).

$$\tau = \frac{R_T}{K_E} \quad (3)$$

The substitution of Eq. (2) with Eq. (1) and Eq. (3) gives Eq. (4).

$$E = E_{MAX} \frac{[A]\tau}{[A](\tau + 1) + K_A} \quad (4)$$

Analysis of OMA

Equation (4) is the equation of OMA². It has three parameters: The equilibrium dissociation constant of agonist (K_A) at the effect-eliciting (active) state of the receptor⁶ that is specific to a combination of ligand and receptor. The maximal possible response of the system (E_{MAX}) is specific to the system. And the “transducer ratio” (τ) that is specific to a combination of ligand and system. Equation (4) is a rectangular hyperbola with the horizontal asymptote, the observed maximal response to agonist A (E'_{MAX}), given by Eq. (5).

$$E'_{MAX} = E_{MAX} \frac{\tau}{\tau + 1} \quad (5)$$

A more efficacious agonist (having a high value of parameter τ) elicits higher E'_{MAX} than less efficacious agonists (having a low value of parameter τ). Thus, τ is actually operational efficacy. The relationship between parameter τ and E'_{MAX} is hyperbolic meaning that two highly efficacious agonists (e.g., τ values 10 and 20) differ in E'_{MAX} values less than two weak agonists (e.g., τ values 0.1 and 0.2).

In Eq. (4), the concentration of agonist A for half-maximal response (EC_{50}), is given by Eq. (6).

$$EC_{50} = \frac{K_A}{\tau + 1} \quad (6)$$

According to Eq. (6), for $\tau > 0$, the EC_{50} value is always lower than the K_A value. The K_A to EC_{50} ratio is greater for efficacious agonists than for weak agonists. Similarly to E'_{MAX} , the relationship between parameter τ and EC_{50} is hyperbolic. In contrast to E'_{MAX} values, the ratio K_A to EC_{50} ratio is more profound for two highly efficacious agonists (e.g., τ values 10 and 20) than for two weak agonists (e.g., τ values 0.1 and 0.2).

Limitations of OMA

The OMA has several weak points. The major drawback of OMA is the lack of physical basis of the agonist equilibrium dissociation constant K_A . Equation (2) assumes that agonist binding [RA] denotes effect-producing active complexes. The agonist binding to the receptor in an inactive conformation is not observed in the response ($K_E \rightarrow \infty$; $\tau = 0$). In the radioligand binding experiments, agonists bind to all receptor conformations including the inactive ones. For various reasons, the receptors in an active conformation may be scarce or absent from radioligand binding experiments. Then it may be impossible to determine the K_A value in the radioligand binding experiments. All three parameters of OMA (E_{MAX} , K_A and τ) are interdependent⁶. To fit Eq. (4) to individual concentration–response curves, one of the parameters must be fixed. E.g., the maximal response of the system E_{MAX} is determined by comparing the functional response to a given agonist in a system with a reduced population of receptors by irreversible alkylation¹⁴ or cell lines with varying receptor expression levels⁶. Alternatively, global fitting of multiple concentration–response curves with all parameters free can be employed. However, due to a high number of degrees of freedom global fitting is less robust than *per partes* methods⁶. Another limitation of the OMA is that the shape of the functional response is a rectangular hyperbola.

Non-hyperbolic OMA

Definition of non-hyperbolic OMA

In practice, concentration–response curves steeper or flatter than the ones described by Eq. (4) are observed. In such cases, Eq. (4) does not fit experimental data. As stated by the authors, Eq. (7) was devised for non-hyperbolic dependence of functional response on the concentration of agonist¹⁰. Eq. (7) was derived in the same way as Eq. (4) from Eq. (1) and Eq. (2) while [RA] and K_E in Eq. (2) were exponentiated to factor n .

$$E = \frac{[A]^n \tau^n E_{MAX}}{[A]^n \tau^n + ([A] + K_A)^n} \quad (7)$$

Analysis of non-hyperbolic OMA

Introduced power factor n changes the slope and shape of the functional-response curve (Supplementary information Figure S3). Nevertheless, Eq. (7) as a mathematical function has rectangular asymptotes: The horizontal asymptote ($x \rightarrow \pm \infty$) E'_{MAX} is given by Eq. (8) and the vertical asymptote ($y \rightarrow \pm \infty$) is equal to $-K_A/(\tau + 1)$ (Supplementary Information Eq. (S2) and Eq. (S3)). From Eq. (7), the EC_{50} value is given by Eq. (9).

$$E'_{MAX} = E_{MAX} \frac{\tau^n}{1 + \tau^n} \quad (8)$$

$$EC_{50} = K_A \frac{1}{\sqrt[n]{2 + \tau^n} - 1} \quad (9)$$

Evidently, the introduced slope factor n affects both the observed maximal response E'_{MAX} and the half-efficient concentration of agonist EC_{50} (Fig. 1A and C). The influence of the slope factor on E'_{MAX} is **bidirectional** (Supplementary Information Table S1, Figure S2). For operational efficacies $\tau > 1$, an increase in the value of the slope factor increases E'_{MAX} . (Figs. 1A and 2A blue lines). For operational efficacies $\tau < 1$, an increase in slope factor decreases E'_{MAX} (Figs. 1C and 2A yellow lines). The effect of the slope factor on E'_{MAX} is the most apparent for low values of operational efficacy τ , making the estimation of model parameters of weak partial agonists impractical. Imagine strong agonist $\tau = 10$ and weak agonist $\tau = 0.1$. For $n = 1$: Strong agonist E'_{MAX} is 90% and weak agonist E'_{MAX} is 10% of system E_{MAX} . For $n = 2$: Strong agonist E'_{MAX} is 99% (one-tenth more) and weak agonist E'_{MAX} is just 1% (ten times less).

An increase in the value of the slope factor increases the EC_{50} value (Fig. 2B). Again, the effect of the slope factor on the EC_{50} value is more eminent at low values of operational efficacy τ (yellow lines). Paradoxically, any combination of operational efficacy τ and slope factor fulfilling the inequality in Fig. 2C (blue area) results in EC_{50} values **greater** than K_A (e.g., Fig. 1C, yellow lines). For example, $EC_{50} > K_A$ applies if $\tau = 0.5$ and $n > 1.6$, or if $\tau = 1$ and $n > 1.6$, or when $\tau = 1.5$ and $n > 2.15$. The upper asymptote of inequality is 2. Thus, the possibility of $EC_{50} > K_A$ applies to $\tau < 2$ in these cases, due to the high slope factor n the response function (Eq. (2)) has a “lag” before the steep growth where the binding function (Eq. (1)) grows faster. Therefore, in this range $EC_{50} > K_A$.

The operational efficacy τ may be also considered as a measure of “receptor reserve”. In a system with a relatively small capacity of a functional response output, the strong agonist reaches its maximal response before reaching full receptor occupancy. Thus, the agonist EC_{50} value is lower than its affinity for the receptor. The smaller the occupancy fraction needed for the full response to a given agonist the greater is difference between agonist EC_{50} and K_A values. According to OMA (Eq. (2)), the relation between EC_{50} and K_A is described by Eq. (6). The greater value of operational efficacy τ , the smaller EC_{50} value and the greater the difference from K_A .

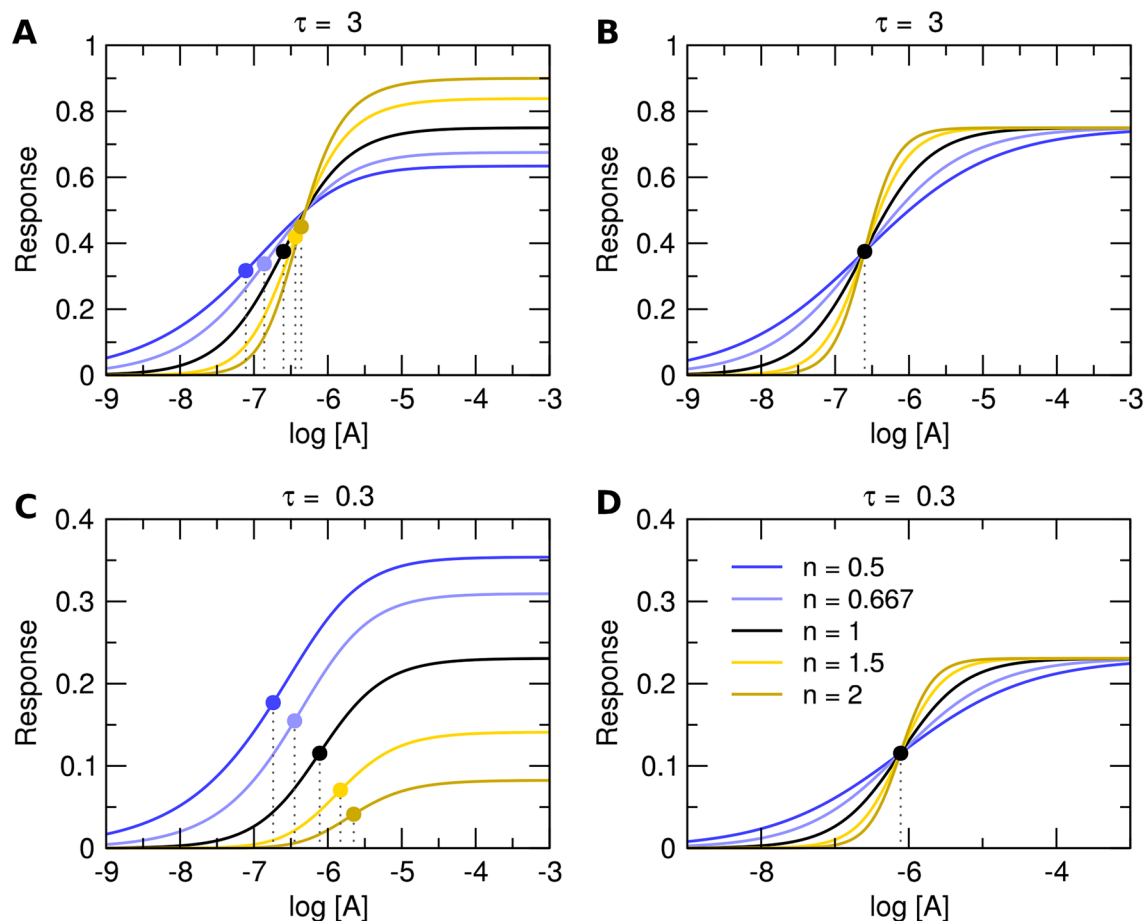


Figure 1. Theoretical concentration–response curves. Theoretical curves of concentration responses under equilibrium according to Eq. (7), left and Eq. (11), right. Simulation parameters: $E_{MAX} = 1$; $\tau = 3$ (top) or $\tau = 0.3$ (bottom); $K_A = 10^{-6}$ M. Values of slope factors are listed in the legend.

Thus, the value of operational efficacy τ is a measure of the receptor reserve of a given agonist in a given system. In a system with a large capacity of functional output, agonists do not have a receptor reserve and must reach full receptor occupancy to elicit a full signal. In such a system, even strong agonists produce small effects attributed to partial agonists. Thus, the parameter τ is specific to a combination of ligand and system.

Nevertheless, for agonists that elicit at least some response in a given system, the parameter τ must be greater than 0. Then according to Eq. (6) of the operational model of agonism, the EC_{50} value must be smaller than the K_A value. In principle, the EC_{50} value greater than the K_A can be achieved only by some parallel mechanism that increases the apparent K_A provided that a ratio of K'_A to K_A is greater than EC_{50} to K_A . For example, such a mechanism may be negative allosteric modulation of agonist binding or non-competitive inhibition of functional response.

Limitations of the non-hyperbolic OMA

Besides all limitations of the hyperbolic OMA, the non-hyperbolic version of OMA has additional drawbacks. The most important is the lack of mechanistic background for factor n . Exponentiation of agonist concentration $[A]$ to power factor n results in non-hyperbolic functional-response curves. Importantly, as shown above, exponentiation of operational efficacy τ to power factor n breaks the logical relationship between observed maximal response E'_{MAX} and operational efficacy τ . That, as it will be shown later, impedes the correct estimation of τ . Further, exponentiation of τ may result in K_A values smaller than EC_{50} (Fig. 2C, blue area).

OMA with Hill coefficient

Definition of OMA with Hill coefficient

The Hill coefficient may serve as an alternative slope factor in the OMA. Hill equation incorporates the Hill coefficient as a slope factor to rectangular hyperbola¹². The major advantage of the Hill coefficient as a slope factor is that it allows for a change in the eccentricity (vertices) of the hyperbola-like curves without changing the centre (EC_{50}) and asymptotes (E'_{MAX}) (Supplementary Information Figure S3). The Hill equation published in 1910¹¹ can be formulated as¹⁵ Eq. (10).

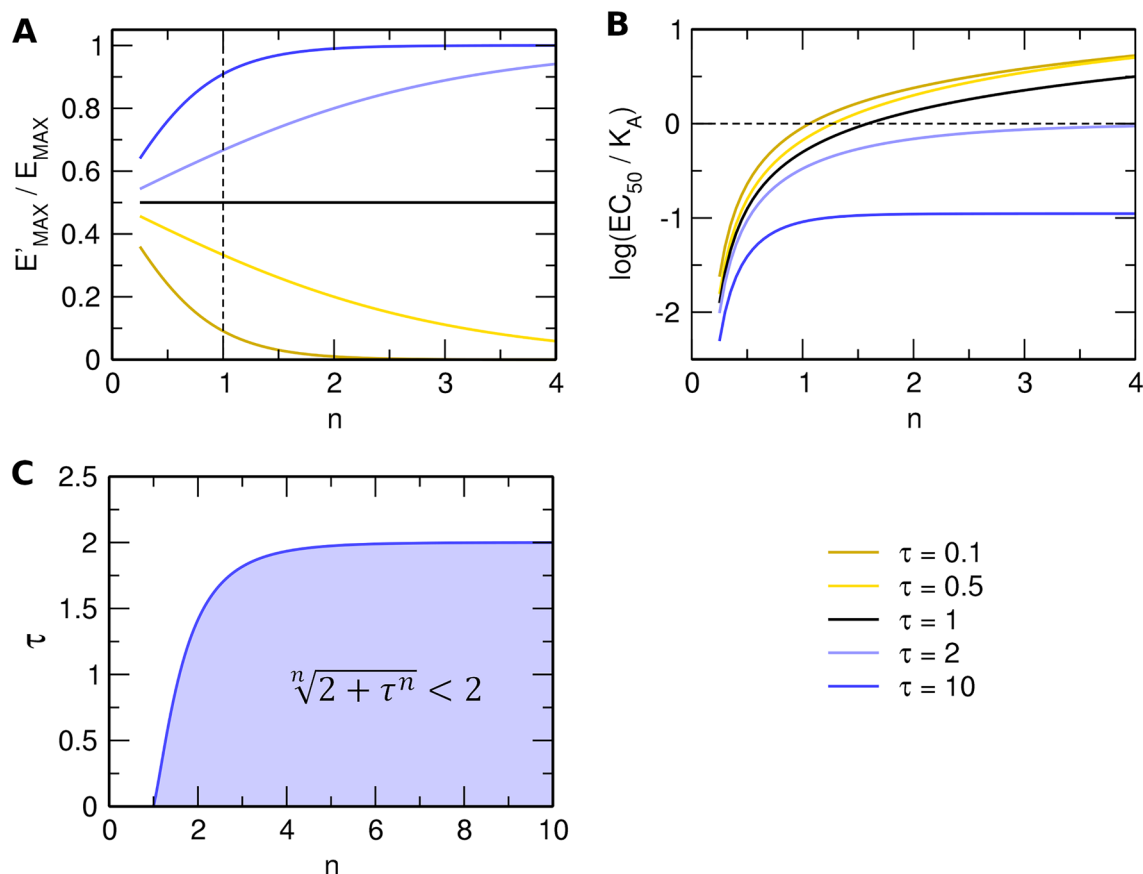


Figure 2. Analysis of Black & Leff equation (Eq. (7)). (A) Dependency of observed E'_{MAX} to system E_{MAX} ratio (ordinate) on slope factor n (abscissa) and operational efficacy τ (legend). (B) Dependency of EC_{50} to K_A ratio (ordinate) on slope factor n (abscissa) and operational efficacy τ (legend). (C) Inequality plot of slope factor n (abscissa) and operational efficacy τ (ordinate) yielding half-efficient concentration EC_{50} greater than equilibrium dissociation constant K_A .

$$E = \frac{[A]^{n_H} E'_{MAX}}{[A]^{n_H} + EC_{50}^{n_H}} \quad (10)$$

where n_H is the Hill coefficient. Substitution of E'_{MAX} by Eq. (5) and EC_{50} by Eq. (6) gives Eq. (11). For derivation from first principles see for example Roche et al.¹⁶

$$E = \frac{[A]^{n_H} \frac{\tau}{\tau+1} E_{MAX}}{[A]^{n_H} + \left(\frac{K_A}{\tau+1}\right)^{n_H}} \quad (11)$$

As expected, the Hill coefficient does not influence the maximal observed response E'_{MAX} or half-efficient concentration of agonist EC_{50} (Fig. 1B,D). Eq. (11) was suggested as suitable for the analysis of functional responses displaying symmetrical response curves¹⁶.

Implications of OMA with Hill coefficient

Analysis of the OMA with slope factor by Black et al. (Eq. (7)) has shown that the slope factor n has a bidirectional effect on the relationship between the parameters E'_{MAX} and τ , and that the slope factor n affects the relationship between the parameters EC_{50} and K_A . In contrast, in Eq. (11) neither the value of E'_{MAX} nor EC_{50} is affected by the Hill coefficient (Fig. 1B,D). The parameters E'_{MAX} and EC_{50} can be readily obtained by fitting Eq. (10) to the single concentration–response data.

Limitations of OMA with Hill coefficient

The major criticism of the Hill equation is its parsimonious character. It is relatively simple and its parameters are easy to estimate. However, as a model, it is just an approximation. In an experiment, the slope of the concentration–response curve different from unity may be a result of the parallel signalling mechanism providing feedback or allosteric cooperativity. In the case of positive cooperativity, it results in steep concentration–response curves. In the case of negative cooperativity, it results in flat concentration–response curves.

OMA of allosteric systems

The simplest scenario leading to variation in the slope of concentration–response curves is allosteric interaction between agonist and allosteric modulator or two molecules of agonist, e.g., in a ligand-gated channel or dimeric GPCR^{17,18}. Positive cooperativity among agonist molecules results in steep functional-response curves and negative cooperativity results in flat functional-response curves. As the mode of cooperativity is the property of a given agonist, the slope of the functional-response curve may vary among agonists. Slope factor **n** in Eq. (7) is deemed the property of the system and thus the same for all agonists. In the attempt to keep slope factor **n** constant in allosteric systems, the second slope factor **m** was introduced to Eq. (7) resulting in¹⁹ Eq. (12):

$$E = \frac{[A]^{nm} \tau^n E_{MAX}}{[A]^{nm} \tau^n + ([A]^m + K_A^m)^n} \quad (12)$$

where factor **n** links agonist concentration to the slope of the functional-response curve and factor **m** links agonist concentration to the slope of the receptor-binding curve. As the slope factors are interdependent one of them must be predetermined. It is only possible to predetermine the slope of the binding curve **m**. When fitting Eq. (12) to the data, functional-response slope factor **n** should become the same for all agonists. Observed maximal response E'_{MAX} is still given by Eq. (8) but half-efficient concentration EC_{50} is given by Eq. (13).

$$EC_{50} = K_A \sqrt[m]{\frac{1}{\sqrt[n]{2 + \tau^n} - 1}} \quad (13)$$

Similarly to Eq. (9), the effect of the binding slope factor **m** on the EC_{50} to K_A ratio depends on operational efficacy τ and functional response slope factor **n**. The effect of binding slope factor **m** depends on the radicand value. The **m**-th root is greater than the radicand when **m** > 1 and radicand > 1 or **m** < 1 and radicand < 1. The **m**-th root is smaller than the radicand when **m** < 1 and radicand > 1 or **m** > 1 and radicand < 1. Moreover, functional responses of allosteric systems may be not only steep or flat but also biphasic including bell-shaped¹⁸. Neither Eq. (7) nor Eq. (12) can accommodate such shapes and equations adequate to the mode of action are needed.

OMA of non-competitive inhibition

As shown in Fig. 2, OMA with slope factor **n** allows for EC_{50} values higher than K_A . The simplest mode of interaction that increases observed EC_{50} above K_A is non-competitive auto-inhibition^{20–23}. Under non-competitive auto-inhibition, RA non-competitively blocks functional response by binding to effector G (Fig. 3). This type of inhibition is characterized by RA binding to a spatially distinct (allosteric) site resulting in a decreased response of effector G. In non-competitive inhibition, RA binds to both sites independently, exerting neutral binding cooperativity (absence of allosteric interaction). Non-competitive auto-inhibition results in a concentration-dependent increase in EC_{50} and a decrease in E'_{MAX} . Functional response is given by Eq. (14).

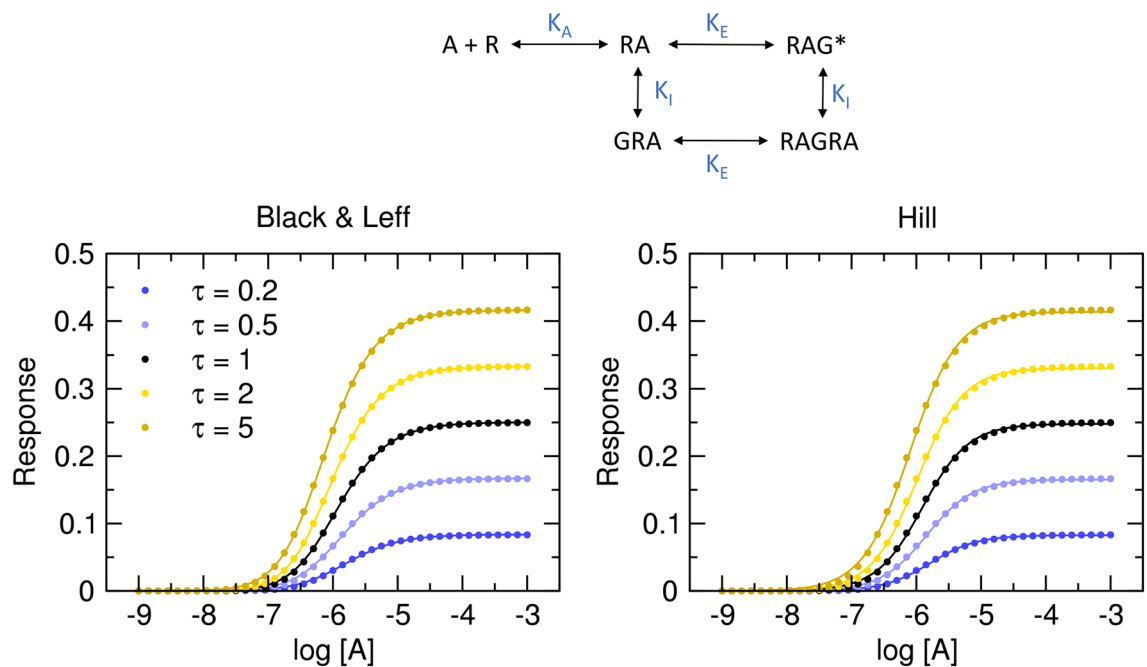


Figure 3. Non-competitive auto-inhibition of functional response. Dots, functional response to an agonist ($K_I = 1$, $E_{MAX} = 1$, $R_T = 1$, $K_A = 10^{-6}$ M) in the model of non-competitive autoinhibition according to Eq. (15). Values of operational efficacies τ are indicated in the legend. Full lines, left, Black & Leff equation (Eq. (7)), right, Hill equation (Eq. (10)) fitted to the data. Parameter estimates are in Table 1.

Model Eqs. 15 and 17					Black & Leff				Hill				Equation 18	
τ	pK_A	K_I	τ'	n	τ	τ^n	pK_A	E'_{MAX}	n_H	pEC_{50}	E'_{MAX}	τ	pK_A	pK_A
0.2	6.00	1	0.091	1.33	0.166	0.0917	5.91	0.084	1.21	5.78	0.083	0.090	5.74	5.99
0.5	6.00	1	0.200	1.46	0.333	0.201	5.98	0.167	1.22	5.84	0.165	0.199	5.76	5.99
1	6.00	1	0.333	1.58	0.499	0.333	6.06	0.250	1.22	5.91	0.248	0.330	5.79	5.99
2	6.00	1	0.500	1.71	0.666	0.499	6.15	0.333	1.21	5.99	0.331	0.494	5.82	6.00
5	6.00	1	0.714	1.55	0.804	0.713	6.15	0.416	1.18	6.10	0.414	0.706	5.87	6.00

Table 1. Results of fitting Black & Leff equations to the model of non-competitive auto-inhibition. Black & Leff (Eq. (7)) and Hill (Eq. (10)) equations were fitted to model data Eq. (15) with E_{MAX} fixed to 1 or E'_{MAX} confined ≤ 1 , respectively.

$$E = E_{MAX} \frac{[RA]}{K_E + [RA]} \frac{[RA]}{K_I + [RA]} \quad (14)$$

For $K_I > 0$, after the substitution of Eq. (1) for [RA], Eq. (14) becomes Eq. (15) (Supplementary information Eq. (S31)).

$$E = E_{MAX} \frac{\tau[A]}{K_A + [A](1 + \tau)} \frac{\sigma[A]}{K_A + [A](1 + \sigma)} \quad (15)$$

where $\sigma = R_T/K_I$. The apparent maximal response E'_{MAX} is given by Eq. (16) (Supplementary Information Eq. (S32)).

$$E'_{MAX} = E_{MAX} \frac{\tau}{1 + \tau} \frac{\sigma}{1 + \sigma} \quad (16)$$

Thus, apparent operational efficacy τ' is given by Eq. (17).

$$\tau' = \frac{\sigma\tau}{\sigma + \tau + 1} \quad (17)$$

The EC_{50} value for the model of non-competitive auto-inhibition is given by Eq. (18) (Supplementary information Eq. (S36)).

$$EC_{50} = K_A \frac{\sqrt{\sigma^2 + 6\sigma\tau + 8\sigma + \tau^2 + 8\tau + 8} + \sigma + \tau + 2}{2(1 + \sigma)(1 + \tau)} \quad (18)$$

Non-competitive auto-inhibition decreases apparent maximal response E'_{MAX} , increases observed half-efficient concentration EC_{50} and results in steep curves (Fig. 3). The resulting concentration–response curve is asymmetric with a typical slope factor of about 1.2 regardless of values of K_I and K_E . Both models fit well. Fitting Hill equation gives correct estimates of apparent maximal response E'_{MAX} and thus correct estimates of apparent operational efficacy τ' (Table 1). In contrast, for $K_I \geq 1$, fitting the Black & Leff equation results in underestimated values of τ and pK_A . Values of τ^n well approximate τ' values.

Fitting Eq. (15) with fixed system E_{MAX} to the model of functional response of non-competitive inhibition yields correct parameter estimates that are associated with the low level of uncertainty only when correct initial estimates of τ and σ are given (Supplementary Information Figure S7 and S8). In the case of $K_I = 5$ (Supplementary Information Figure S9), estimates of operational efficacy τ and inhibition factor σ are swapped pointing to the symmetry of Eq. (15). This symmetry makes calculation of τ and σ impossible as any τ and σ combination resulting in an appropriate apparent efficacy τ' (Eq. (17)) corresponds well to a given functional-response data (Supplementary Information Figure S8). Fitting the Black & Leff equation (Eq. (7)) yields wrong estimates of K_A and underestimated values of τ . Importantly, the extent of underestimation varies. The τ of 0.2 was underestimated by 17%. The τ of 5 was underestimated sixfold. In contrast, the calculation of apparent operational efficacies from the fitting of the Hill equation (Eq. (10)) is very close.

Signalling feedback

Signalling feedback occurs when outputs of a system are routed back as inputs²⁴. Negative feedback is a very common auto-regulatory (auto-inhibitory) mechanism in nature, for example at G-protein coupled receptors²⁵. Positive feedback also occurs in biology to propagate signals that would be otherwise dampened by other mechanisms, e.g. neuronal action potential. In the receptor-effector systems, an increase in output signal [RAG] proportionally either decreases (negative feedback) or increases (positive feedback) input [RA]²⁶. Functional response in employing feedback mechanisms is then given by Eq. (19). For derivation see Supplementary Information Eqs. (S25) to (S37).

$$E = E_{MAX} \frac{\tau[A](\tau[A] + [A] + K_A)}{[A]^2(\delta\tau + \tau^2 + \tau + 1) + [A]K_A(\delta\tau + \tau + 2) + K_A^2} \quad (19)$$

where δ is a feedback factor. Values greater than 1 denote negative feedback. Values smaller than 1 denote positive feedback. The maximal response E'_{MAX} to an agonist with operational efficacy τ is related to the maximal response of the system E_{MAX} according to Eq. (20).

$$E'_{MAX} = E_{MAX} \frac{\tau^2 + \tau}{\delta\tau + \tau^2 + \tau + 1} \tag{20}$$

Negative feedback decreases the observed maximal response to an agonist E'_{MAX} while positive feedback increases it. And apparent operational efficacy τ' of a given agonist can be calculated according to Eq. (21).

$$\tau' = \frac{\tau^2 + \tau}{\delta\tau + 1} \tag{21}$$

Furthermore, negative feedback decreases the K_A to EC_{50} ratio while positive feedback increases it (Supplementary Information Eq. (S54)). For derivations see Supplementary Information Eq. (S37) through Eq. (S54). In general, negative feedback results in flat functional-response curves as with the increase in signal output proportionally more of an agonist is needed for the same increase of the signal. Conversely, positive feedback results in steep functional-response curves as signal output proportionally increases signal input (Supplementary Information Figure S9).

Importantly, in a system with constant negative feedback, like in Fig. 4, the steepness of the curve depends on operational efficacy τ . Functional-response curves to agonists with high operational efficacy are flatter than the ones of agonists with low operational efficacy (Table 2).

Fitting Eq. (19) with fixed system E_{MAX} to the model employing feedback mechanisms yields correct parameter estimates that are associated with the low level of uncertainty when correct initial estimates of τ and δ are

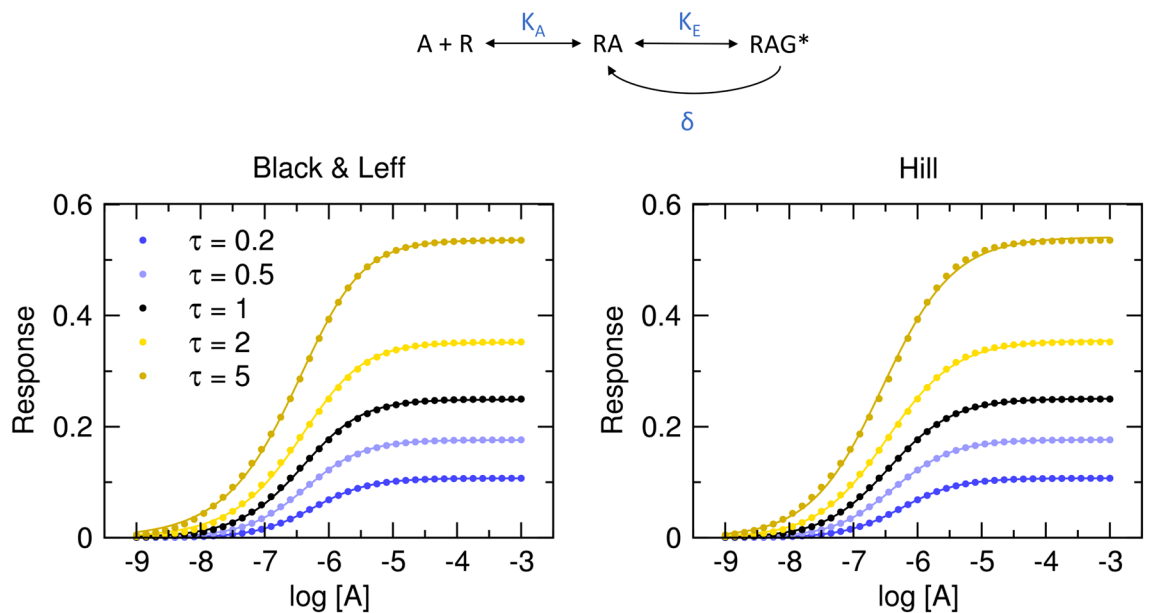


Figure 4. Functional response with signal feedback. Dots, functional response to an agonist ($E_{MAX}=1$, $R_T=1$, $K_A=10^{-6}$ M) in the model of the system with constant negative feedback ($\delta=5$) according to Eq. (19). Values of operational efficacies τ are indicated in the legend. Full lines, left, Black & Leff equation (Eq. (7)), right, Hill equation (Eq. (10)) fitted to the data. Parameter estimates are in Table 2.

Model Eqs. 19 and 21				Black & Leff					Hill					Eq. S42
τ	pK_A	δ	τ'	n	τ	τ^n	pK_A	E'_{MAX}	n_H	pEC_{50}	E'_{MAX}	τ	pK_A	pK_A
0.2	6.00	5	0.120	0.96	0.109	0.119	6.17	0.106	0.98	6.25	0.107	0.120	6.20	6.01
0.5	6.00	5	0.214	0.87	0.168	0.212	6.20	0.175	0.93	6.38	0.177	0.214	6.30	6.01
1	6.00	5	0.333	0.76	0.236	0.334	6.13	0.250	0.87	6.45	0.251	0.333	6.33	6.02
2	6.00	5	0.545	0.68	0.409	0.544	6.01	0.353	0.81	6.48	0.355	0.545	6.29	6.01
5	6.00	5	1.154	0.66	1.245	1.16	5.86	0.536	0.78	6.55	0.541	1.155	6.22	6.01

Table 2. Results of fitting Black & Leff equations to the model of the system employing signalling feedback. Black & Leff (Eq. (7)) and Hill (Eq. (10)) equations were fitted to model data with E_{MAX} fixed to 1 or E'_{MAX} confined ≤ 1 , respectively.

given (Supplementary Information Figure S9 and S10). Fitting the Black & Leff equation (Eq. (7)) yields wrong estimates of K_A and underestimated values of τ . Again, the extent of underestimation varies. The τ of 0.2 was underestimated by 67%. The τ of 5 was underestimated fourfold. However, values of τ^n well approximate τ values. In contrast, calculations of apparent operational efficacies from the fitting of the Hill equation (Eq. (10)) are very close.

Systems with a similar expression of receptor and effector ($[R_T] \approx [G_T]$)

The Eq. (2) and consequently Eq. (4) are valid only when either $[RA]$ or $[G]$ is constant. That requires $[R_T] \gg [G_T]$ or $[R_T] \ll [G_T]$. Usually, systems exhibit receptor reserve, indicating $[R_T] \gg [G_T]$. In systems with low receptor expression, $[R_T]$ and $[G_T]$ may be similar. In a such system $[RAG]$ as a function of $[RA]$ is given by Eq. (22) (Supplementary Information Eq. (S62)).

$$[RAG] = \frac{1}{2} \left(K_E + [RA] + [G_T] - \sqrt{K_E^2 + 2K_E([RA] + [G_T]) + ([RA] - [G_T])^2} \right) \quad (22)$$

where $[RA]$ denotes the concentration of all receptor agonist complexes, free RA plus RA in complex with G (RAG) (Supplementary Information Eq. (S56)). $[RAG]$ as a function of $[A]$ (Supplementary Information Eq. (S64)) has only approximate solutions. Therefore, $[RA]$ values as a function of $[A]$ were calculated as $[RA]$ according to Eq. (1) and used in Eq. (22) to model functional responses of the system with low receptor-expression level (Fig. 5). The resulting curves are steep and asymmetric. In the low receptor-expression system, the response reaches the maximum at lower agonist concentration due to receptor depletion that cuts off the signal early which results in an apparent increased steepness and, in turn, in a curve asymmetry. The greater the operational efficacy is, the steeper and more asymmetric functional-response curves are (Table 3). However, the observed operational efficacy τ is equal to the modelled operational efficacy.

Fitting the Black & Leff equation (Eq. (7)) to the model system with a low receptor-expression level yields wrong estimates of K_A for extremely high operational efficacy ($\tau = 1000$). Values of τ are far off for all modelled efficacies. While τ of 1000 is overestimated more than sixfold, the other τ values are underestimated up to

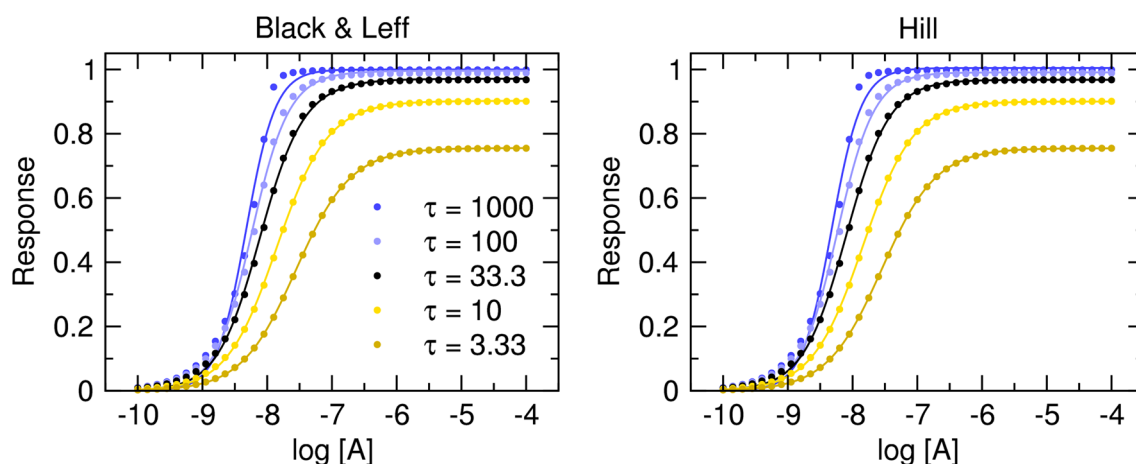


Figure 5. Functional response of the system with a similar expression of receptor and effector ($[R_T] \approx [G_T]$). Dots, functional-response data modelled in two steps. First, binding was calculated according to Eq. (1). Then resulting $[RA]$ was used in Eq. (22). $E_T = 10^{-6}$ M, $R_T = 10^{-5}$ M, $K_A = 10^{-7}$ M. Values of operational efficacies τ are indicated in the legend. Full lines, left, Black & Leff equation (Eq. (7)), right, Hill equation (Eq. (10)) fitted to the data. Parameter estimates are in Table 3.

Model Eqs. 1 and 22			Black & Leff				Hill				
τ	pK_A	n	τ	τ^n	pK_A	E'_{MAX}	n_H	pEC_{50}	E'_{MAX}	τ	pK_A
1000	7.00	1.91	6701	$2.03 \cdot 10^7$	4.50	1.00	1.89	8.32	1.00	CNBD	CNBD
100	7.00	1.54	36.2	251	6.68	0.996	1.52	8.23	0.991	108	6.19
33.3	7.00	1.35	13.6	33.9	6.98	0.971	1.29	8.10	0.968	30.1	6.61
10	7.00	1.15	6.94	9.28	6.98	0.903	1.11	7.84	0.900	9.04	6.84
3.33	7.00	1.05	2.93	3.09	6.98	0.756	1.03	7.55	0.755	3.08	6.94

Table 3. Results of fitting Black & Leff equations to the model of the system with a similar expression of receptor and effector ($[R_T] \approx [G_T]$). Black & Leff (Eq. (7)) and Hill (Eq. (10)) equations were fitted to model data with E_{MAX} fixed to 1 or E'_{MAX} confined ≤ 1 , respectively. CNBD cannot be determined.

threefold. Values of τ^n approximate model τ values of 33.3, 10 and 3.33. However, the τ^n value is overestimated 20,000 and 2.5 times for model values of 1000 and 100, respectively. Except for the τ value of 1000, operational efficacies calculated according to the Hill equation (Eq. (10)) are less than 10% off the model values.

The case study

How fitting the Black & Leff equation to experimental data can affect estimates of the operational efficacy and subsequent analysis is demonstrated in the following example of measurement of the GTP γ S binding as a functional response of M₂ receptor to muscarinic agonists carbachol, iperoxo, N-desmethyl clozapine (NDMC) and oxotremorine at five subtypes of inhibitory G-proteins: G_{i1}, G_{i2}, G_{i3}, G_{oA} and G_{oB} expressed in Sf9 cells. According to the saturation of [³H]NMS binding, Sf9 cell membranes contained about 7 pmol of binding sites per mg of membrane protein. Co-expression of individual subtypes of inhibitory G-proteins did not affect the expression level of M₂ receptors. According to competition with [³H]NMS binding, tested agonists had the same affinity for M₂ receptors in all co-expression systems (Supplementary Information Table S2).

When analysing the functional response, first, system E_{MAX} values were determined using the procedure described earlier⁶. They ranged from 84 to 88% of the maximum binding capacity of G-proteins. After subtraction of basal binding, responses were expressed as a fraction of E_{MAX}. The system E_{MAX} was set equal to 1.

Signalling profiles varied among subtypes of G-proteins. For example, carbachol and oxotremorine reached similar maximal responses E'_{MAX} at G_{i1}, G_{oA} and G_{oB}. At G_{i2}, the E'_{MAX} of oxotremorine was substantially greater than the E'_{MAX} of carbachol. In contrast, at G_{i3}, the E'_{MAX} of oxotremorine was substantially lower than the E'_{MAX} of carbachol (Fig. 6). Also, the steepness of functional responses to agonists varied among agonists as well as among subtypes of G-proteins. The functional response to carbachol was normal ($n_H \approx 1$), except for a flat response ($n_H = 0.68$) at G_{oB} (Supplementary information Table S2). The functional response to NDMC was steep ($n_H > 1.2$) at G_{i1} and G_{i3}, normal at G_{i2} and flat ($n_H < 0.85$) at G_{oA} and G_{oB}. As the exact reason for variation in the steepness of functional-response curves is unknown, the Hill equation (Eq. (11)) was fitted to the experimental data for comparison with the fitting of the Black & Leff equation (Eq. (7)). Results of fitting are summarized in Supplementary Information Table S2).

The analysis of estimates of equilibrium dissociation constants K_A obtained from fitting Black & Leff (Eq. (7)) and Hill (Eq. (11)) equations shows that in comparison to Hill fits, estimates from Black & Leff fits are associated with greater variability (among individual fits) and uncertainty (individual fits) (Fig. 7). In the majority of cases, K_A estimates according to the Black & Leff equation were substantially lower than according to the Hill equation. Except for NDMC, K_A estimates for both models are higher than K_I from competition with [³H]NMS.

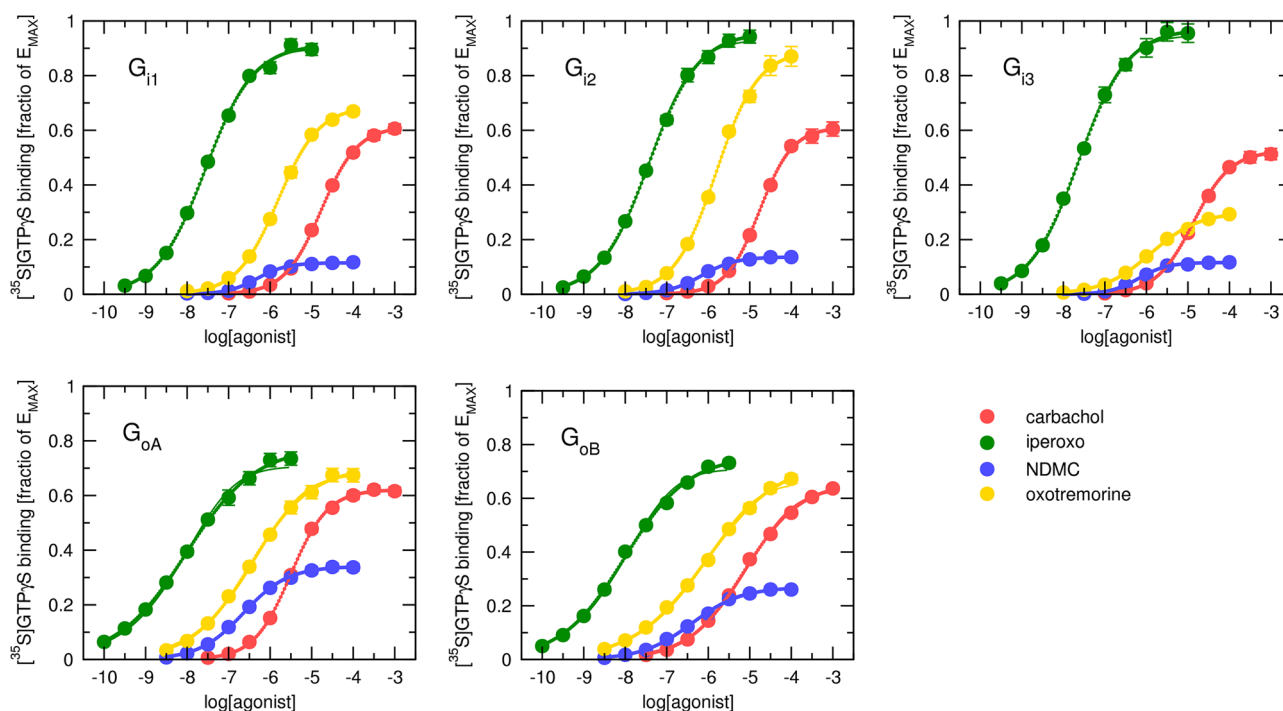


Figure 6. Functional response of muscarinic M₂ receptors. GTP γ S binding to G_{i1} (upper left), G_{i2} (upper middle), G_{i3} (upper right) G_{oA} (lower left) and G_{oB} (lower right) G-proteins upon stimulation of M₂ muscarinic receptors by carbachol (red), iperoxo (green), NDMC (blue) or oxotremorine (yellow) at the concentration indicated on the x-axis is expressed as the fraction of maximal response of the system (E_{MAX}). Data are means \pm SD from 3 to 5 independent experiments performed in quadruplicates. Solid curves, Black & Leff equation (Eq. (7)). Dotted curves, Hill equation (Eq. (11)). Parameter estimates are in Supplementary Information Table S2.

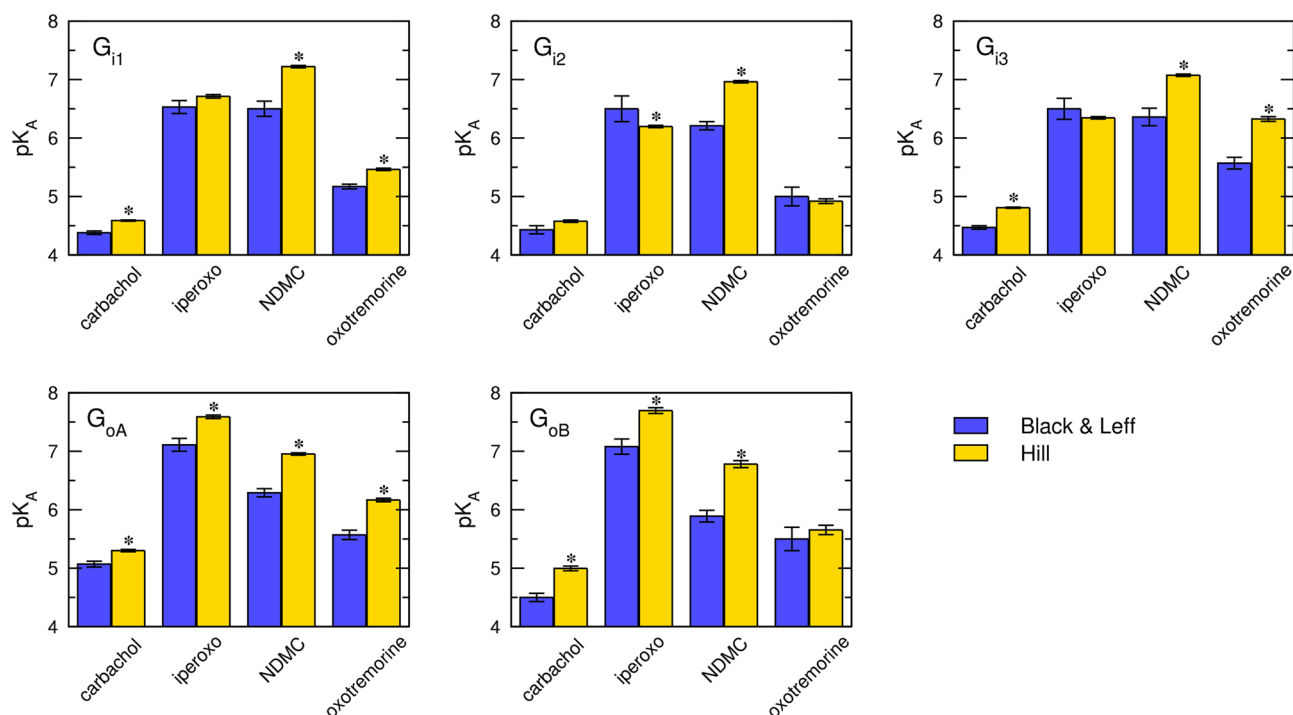


Figure 7. Analysis of pK_A estimates. Estimates of equilibrium dissociation constant K_A from fitting Black & Leff (Eq. (7)) (blue) or Hill (Eq. (11)) (yellow) equation are expressed as negative logarithms (pK_A). Data are means \pm SD from fits of 5 independent experiments performed in quadruplicates. *, different from Black & Leff ($p < 0.05$) according to ANOVA and Tukey HSD post-test.

Notably, agonist K_i values are the same for all subtypes of G-protein α -subunit while K_A values vary among them (Supplementary Information Table S2 and S3).

Similarly to estimates of K_A , in comparison to Hill fits, estimates of operational efficacies τ from Black & Leff fits are associated with greater variability and uncertainty (Fig. 8). Overall, τ values tend to be underestimated for flat curves and overestimated for steep curves. Following analysis of the Black & Leff equation, this phenomenon is apparent for low operational efficacies, especially for $\tau < 1$. In the extreme case of steep response to NDMC ($n = 1.5$) and flat response to oxotremorine ($n = 0.7$) at G_{i3} , Black & Leff estimates of τ are the same for both agonists despite oxotremorine elicited E'_{MAX} three-times higher than NDMC. In the less extreme case, at G_{oB} G-protein, oxotremorine was about 60% more efficacious than carbachol but estimated τ values by Black & Leff were the same for both agonists although functional-response curves of both agonists are flat ($n_H = 0.6$ and 0.5 , respectively). Thus, even a small change in the steepness of the functional-response curve has a profound effect on the estimation of the τ value.

Discussion

The operational model of agonism (OMA)² is widely used in the evaluation of agonism. The OMA characterizes a functional response to an agonist by the equilibrium dissociation constant of the agonist (K_A), the maximal possible response of the system (E_{MAX}) and the operational efficacy of the agonist (τ) (Eq. (4)). To fit non-hyperbolic functional responses slope factor n was introduced to the OMA (Eq. (7))¹⁰. Analysis of the Black & Leff equation (Eq. (7)) has shown that the slope factor n has a bidirectional effect on the relationship between the parameters E'_{MAX} and τ (Fig. 1A versus C) and also affects the relationship between the parameters EC_{50} and K_A .

Fitting Black & Leff equation (Eq. (7)) to the models of non-competitive auto-inhibition (Fig. 3, Table 1), signalling feedback (Fig. 4, Table 2) and system with a similar expression of receptor and effector ($[R_T] \approx [G_T]$) (Fig. 5, Table 3) resulted in inaccurate estimates of τ and K_A values. In the presented examples, the degree of over- or under-estimation of τ is not the same for all its values but depends on the value of τ , distorting relations among estimates of τ values. In contrast, fitting the Hill equation (Eq. (10)) to the model data gave more or less accurate estimates of apparent operational efficacies τ' from which operational efficacies can be calculated (according to Eq. (17), and Eq. (21)), provided that mechanism of action is known.

Biased agonists stabilize specific conformations of the receptor leading to non-uniform modulation of individual signalling pathways²⁷. To measure an agonist bias, the parameters τ and K_A must be determined and $\log(\tau/K_A)$ values of tested and reference agonists compared at two signalling pathways³. It is evident from the analysis of the Black & Leff equation, that as far as the EC_{50} value is dependent on parameters n and τ (Fig. 1A,C), $\log(\tau/K_A)$ values cannot be compared to judge possible signalling bias unless the parameter n is equal to 1 for both tested and reference agonist.

Despite the dire effects of slope factor n , the Black & Leff equation is widely accepted^{4,28–34}. It even entered textbooks⁵. Very little concern on factor n has risen. For example, Kenakin et al.³ analysed in detail the effects

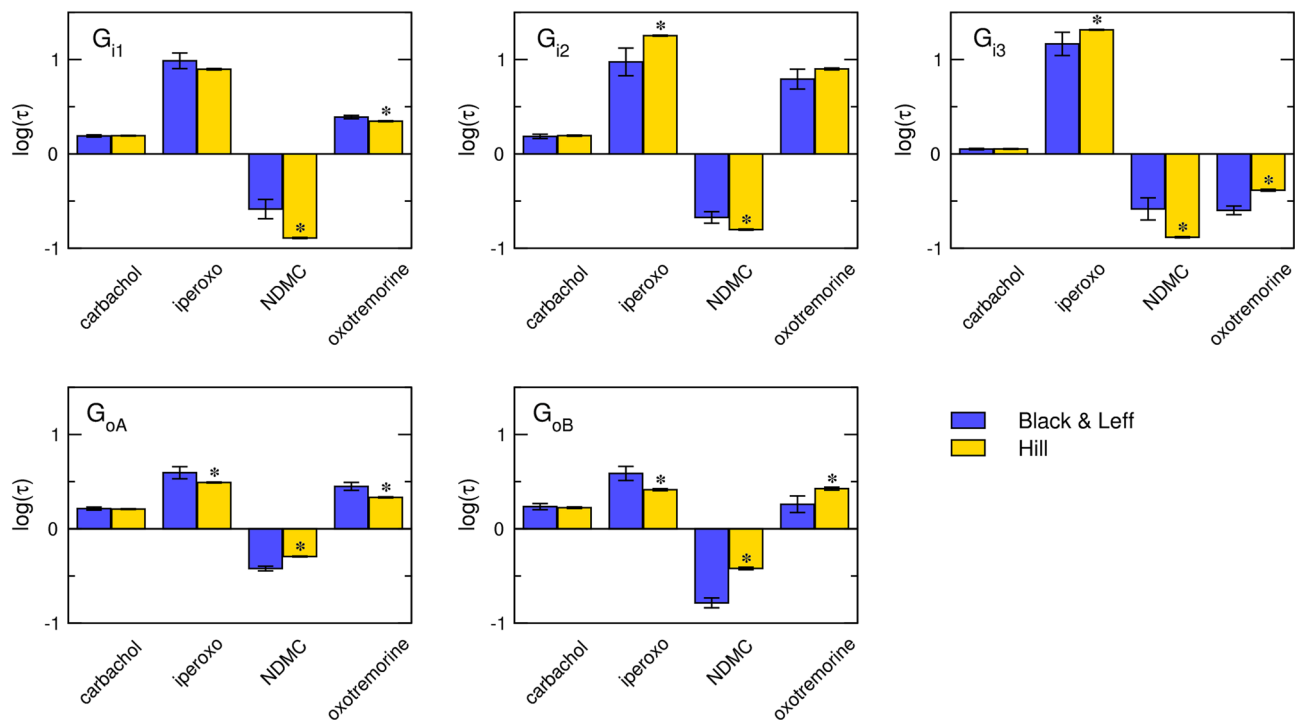


Figure 8. Analysis of τ estimates. Estimates of operational efficacy τ from fitting Black & Leff (Eq. (7)) (blue) or Hill (Eq. (11)) (yellow) equation are expressed as decadic logarithms ($\log \tau$). Data are means \pm SD from fits of 5 independent experiments performed in quadruplicates. *, different from Black & Leff ($p < 0.05$) according to ANOVA and Tukey HSD post-test.

of slope factor n on EC_{50} and τ to K_A ratio but did not deal with the bi-directional effect of n on τ nor proposed an alternative approach to avoid potential pitfalls. To force a proper shape on functional-response curves whilst keeping slope factor n constant for all ligands, Gregory et al.¹⁹ introduced the second slope factor into their OMA and operational model of allosterically modulated agonism (OMAMA) analysis making equations even more complex. So far, the greatest criticism of OMA was voiced by Roche et al.¹⁶, noting that to accommodate the shape of theoretical curves Black & Leff equation tends to overestimate equilibrium dissociation constant K_A and operational efficacy τ and thus be misleading. They advocated for different expressions of operational models including OMA modified by the Hill coefficient in the case of symmetric concentration-response curves. Theoretical models show that in cases of non-competitive auto-inhibition and signal feedback where the slope of functional response does not vary, Black & Leff equation can be used to estimate apparent operational efficacy τ' (Tables 1 and 2). However, estimates of operational efficacy do not approximate τ of the models.

The fitting of the Hill equation (Eq. (10)) to the functional response is straightforward and easier than fitting the Black & Leff equation. As shown in Figs. 3, 4, 5, 6, the Hill equation fits well with various functional-response curves, often better than the Black & Leff equation. In contrast to the Black & Leff equation, the Hill equation gives correct estimates of maximal response to agonist E'_{MAX} and its half-efficient concentration EC_{50} as documented in Tables. 1, 2, 3 and Figs. 7 and 8. In the case of the Hill equation, neither the value of E'_{MAX} nor the value of EC_{50} is affected by the Hill coefficient (Fig. 1B,D). Therefore, biased signalling may be inferred from the comparison of the ratio of intrinsic activity (E'_{MAX}/EC_{50}) of tested agonist to the intrinsic activity of reference agonist at two signalling pathways as in the case of the Hill equation the E'_{MAX}/EC_{50} ratio is equivalent to τ/K_A ratio^{35,36}. Further, if needed, apparent operational efficacy τ' can be calculated from known E'_{MAX} values and known maximal response of the system E_{MAX} . From the relationship between τ' and EC_{50} ^{6,17}, the mechanism of functional response can be inferred by comparison to explicit models.

The case study of the functional response of individual subtypes of inhibitory G-proteins to activation of the M_2 muscarinic receptor (Fig. 6) demonstrated the pitfalls of exponentiation of operational efficacy τ : At G_{i3} G-protein, oxotremorine reached 3-times higher maximal response E'_{MAX} than NDMC. However, estimates of operational efficacy τ by the Black & Leff equation were the same for both agonists (Fig. 8), rendering it unsuitable for such data. An analysis of the Black & Leff equation implies that the source of the discrepancy lies in the profound effects of slope factor n on the estimation of τ value. The τ estimates by the Hill equation reflected differences in E'_{MAX} values, making it suitable for such a scenario. The root of the problem is variation in the slope of the functional response among tested agonists, indicating that the slope is not the property of the system required by the Black & Leff model. Rather agonists exert various degrees of cooperativity. As muscarinic receptors possess only one orthosteric binding site the data indicate that muscarinic receptors may function as oligomers¹⁸. Although cooperativity does not automatically mean oligomerization³⁷, several lines of evidence indicate that muscarinic receptors may indeed oligomerize^{38–41}.

Conclusions

Analysis of the Black & Leff equation has shown that (i) The slope factor n has a bidirectional effect on the relationship between the parameters E'_{MAX} and τ . (ii) The slope factor n affects the relationship between the parameters EC_{50} and K_A . Fitting the Black & Leff equation gives wrong estimates of τ and K_A values when slope factor n varies among concentration–response curves, limiting the use of the Black & Leff equation to evaluate concentration–response curves with the same slope. Analysis of the Hill equation has shown that the Hill coefficient does not affect the relationship between the parameters E'_{MAX} and τ nor between the parameters EC_{50} and K_A . Fitting the Black & Leff equation to the experimental data demonstrated the drawbacks of exponentiation operational efficacy τ . In contrast, fitting the Hill equation to the experimental data gave more realistic estimates of K_A and τ . Black & Leff equation may be safely used only for systems where the slope of functional response does not vary substantially to estimate apparent operational efficacy.

Methods

Models and equations

Models and equations were derived from scratch as described in Supplementary Information. For modelling the theoretical curves and fitting curves to the experimental data the Python code employing numpy, scipy and matplotlib libraries was written.

Preparation of cells and membranes

Spodoptera frugiperda cells (Sf9) (Gibco) were maintained as a suspension culture in serum-free insect cell growth medium SF900 III (Gibco) in a plastic Erlenmeyer flask in a shaking incubator at 27 °C and 135 rpm in a non-humidified environment. The cultures were maintained at a density of $1\text{--}4 \times 10^6$ cells/ml. The density of the cells was determined with a haemocytometer, and viability was assessed by the exclusion of 0.2% trypan blue (Sigma-Aldrich). Human M_2 receptors and α -subunits of (G_{i1} , G_{i2} , G_{i3} , G_{oA} or G_{oB}) G-proteins were expressed in recombinant baculoviruses, which were constructed and generated according to Bac-to-Bac[®] Baculovirus Expression System manual (Life Technologies)⁴².

One hundred ml of Sf9 cell suspension at a density of 2×10^6 cells/ml were co-infected with baculoviruses encoding the M_2 receptor and G_o or G_i α -subunit at a multiplicity of infection MOI = 0.1: 0.1. All infections were allowed to proceed for 69 h. Infected cells were harvested by centrifugation at $500 \times g$ for 5 min and frozen at -80 °C.

The pellets of harvested cells were suspended in the ice-cold homogenization medium (100 mM NaCl, 20 mM Na-HEPES, 10 mM EDTA, pH = 7.4) and homogenized on ice by two 30 s strokes using a Polytron homogenizer (Ultra-Turrax; Janke & Kunkel GmbH & Co. KG, IKA-Labortechnik, Staufen, Germany) with a 30-s pause between strokes. Cell homogenates were centrifuged for 5 min at $1000 \times g$. The supernatant was collected and centrifuged for 30 min at $30,000 \times g$. Pellets were suspended in the washing medium (100 mM NaCl, 10 mM $MgCl_2$, 20 mM Na-HEPES, pH = 7.4), left for 30 min at 4 °C, and then centrifuged again for 30 min at $30,000 \times g$. The resulting membrane pellets were kept at -80 °C until assayed.

[³H]NMS binding

Membranes (approximately 10 μg of membrane proteins per sample) from Sf9 cells were incubated in 96-well plates for 3 (saturation) or 5 h (competition) at 25 °C in the incubation medium (100 mM NaCl, 20 mM Na-HEPES, 10 mM $MgCl_2$, pH = 7.4). The incubation volume for competition and saturation experiments with [³H]NMS was 400 μl or 800 μl , respectively.

In saturation experiments, eight concentrations of the [³H]NMS ranging from 94 to 1000 pM were used. Agonist binding was determined in competition experiments with 1 nM [³H]NMS. Nonspecific binding was determined in the presence of 10 μM unlabelled atropine. Incubation was terminated by filtration through Whatman GF/C glass fibre filters (Whatman) using a Brandel harvester (Brandel, USA). Filters were dried in a microwave oven (3 min, 800 W), and then solid scintillator Meltilex A was melted on filters (105 °C, 90 s) using a hot plate. The filters were cooled and counted in a Wallac Microbeta scintillation counter (Wallac, Finland).

GTP γ S binding

Agonist-stimulated [³⁵S]GTP γ S binding was performed as currently described⁴³. Briefly, it was performed in 96-well plates at 30 °C in the incubation medium described above that was supplemented with freshly prepared dithiothreitol at a final concentration of 1 mM. Suspension of membranes of Sf9 cells expressing M_2 + G-protein α -subunit were preincubated with GDP and agonists for 15 min, then [³⁵S]GTP γ S was added for an additional 20 min. The final concentration of GDP and [³⁵S]GTP γ S was 20 μM and 500 pM, respectively. The maximum binding capacity of G-proteins was determined in the absence of GDP. Nonspecific binding was determined in the presence of 1 μM non-labelled GTP γ S. Incubations were terminated by filtration through GF/C filtration plates (Millipore) using a Brandel cell harvester (Perkin Elmer, USA). Plates were dried in a microwave oven at 800W for 3 min and then 40 μl of ROTISZINT[®] Eco Plus (ROTH) was added. The plates were counted in the Wallac Microbeta scintillation counter.

Analysis of experimental data

Experimental data were analysed using the two-step procedure described earlier^{6,17}. First, the maximum system response E_{MAX} was determined. After subtracting the value of the basal signal, functional responses were expressed as the fraction of corresponding E_{MAX} . Then, the Hill equation (Eq. (10)) and the Black & Leff equation

(Eq. (7)) were fitted to the data. In the case of the Hill equation, the maximum response to an agonist E'_{MAX} was confined to less than 1. In the case of the Black & Leff equation, system E_{MAX} was set equal to 1.

Data availability

The data that support the findings of this study are available from the corresponding author upon reasonable request.

Received: 30 May 2023; Accepted: 14 October 2023

Published online: 16 October 2023

References

- Stephenson, R. P. A modification of receptor theory. *Br. J. Pharmacol. Chemother.* **11**, 379–393 (1956).
- Black, J. W. & Leff, P. Operational models of pharmacological agonism. *Proc. R. Soc. London. Ser. B Biol. Sci.* **220**, 141–162 (1983).
- Kenakin, T., Watson, C., Muniz-Medina, V., Christopoulos, A. & Novick, S. A simple method for quantifying functional selectivity and agonist bias. *ACS Chem. Neurosci.* **3**, 193–203 (2012).
- Kenakin, T. & Christopoulos, A. Signalling bias in new drug discovery: detection, quantification and therapeutic impact. *Nat. Rev. Drug Discov.* **12**, 205–216 (2013).
- Kenakin, T. P. Agonists: The Measurement of Affinity and Efficacy in Functional Assays. In *A Pharmacology Primer* 85–117 (Academic Press, 2014). doi:<https://doi.org/10.1016/b978-0-12-407663-1.00005-3>.
- Jakubík, J. *et al.* Applications and limitations of fitting of the operational model to determine relative efficacies of agonists. *Sci. Rep.* **9**, 4637 (2019).
- Hall, D. A. & Giraldo, J. A method for the quantification of biased signalling at constitutively active receptors. *Br. J. Pharmacol.* **175**, 2046–2062 (2018).
- Onaran, H. O. *et al.* Systematic errors in detecting biased agonism: Analysis of current methods and development of a new model-free approach. *Sci. Rep.* **7**, 44247 (2017).
- Onaran, H. O. & Costa, T. Conceptual and experimental issues in biased agonism. *Cell. Signal.* **82**, 109955 (2021).
- Black, J. W., Leff, P., Shankley, N. P. & Wood, J. An operational model of pharmacological agonism: the effect of $E/[A]$ curve shape on agonist dissociation constant estimation. *Br. J. Pharmacol.* **84**, 561–571 (1985).
- Hill, A. V. The possible effects of the aggregation of the molecules of haemoglobin on its dissociation curves. *J. Physiol.* **40**, i–vii (1910).
- Gesztelyi, R. *et al.* The Hill equation and the origin of quantitative pharmacology. *Arch. Hist. Exact Sci.* **66**, 427–438 (2012).
- Clark, A. J. The antagonism of acetyl choline by atropine. *J. Physiol.* **61**, 547–556 (1926).
- Furchgott, R. F. The use of β -haloalkylamines in the differentiation of receptors and in the determination of dissociation constants of receptor-agonist complexes. *Adv. Drug Res.* **3**, 21–55 (1966).
- Weiss, J. N. The Hill equation revisited: Uses and misuses. *FASEB J.* **11**, 835–841 (1997).
- Roche, D., van der Graaf, P. H. & Giraldo, J. Have many estimates of efficacy and affinity been misled? Revisiting the operational model of agonism. *Drug Discov. Today* **21**, 1735–1739 (2016).
- Jakubík, J., Randáková, A., Chetverikov, N., El-Fakahany, E. E. & Doležal, V. The operational model of allosteric modulation of pharmacological agonism. *Sci. Rep.* **10**, 14421 (2020).
- Jakubík, J. & Randáková, A. Insights into the operational model of agonism of receptor dimers. *Exp. Opin. Drug Discov.* **17**, 1181–1191 (2022).
- Gregory, K. J., Giraldo, J., Diao, J., Christopoulos, A. & Leach, K. Evaluation of operational models of agonism and allosterism at receptors with multiple orthosteric binding sites. *Mol. Pharmacol.* **97**, 35–45 (2020).
- Strelow, J. *et al.* *Mechanism of Action Assays for Enzymes. Assay Guidance Manual* (2004).
- Ogawa, H., Sato, M. & Yamashita, S. Gustatory impulse discharges in response to saccharin in rats and hamsters. *J. Physiol.* **204**, 311–329 (1969).
- Alberts, P., Bartfai, T. & Stjärne, L. Site(s) and ionic basis of alpha-autoinhibition and facilitation of 3H noradrenaline secretion in guinea-pig vas deferens. *J. Physiol.* **312**, 297–334 (1981).
- Li, S.-J. *et al.* Cooperative autoinhibition and multi-level activation mechanisms of calcineurin. *Cell Res.* **26**, 336–349 (2016).
- Del Vecchio, D. & Murray, R. M. *Biomolecular Feedback Systems. Biomolecular Feedback Systems* (Princeton University Press, 2014). doi:<https://doi.org/10.23943/princeton/9780691161532.001.0001>.
- Black, J. B., Premont, R. T. & Daaka, Y. Feedback regulation of G protein-coupled receptor signaling by GRKs and arrestins. *Semin. Cell Dev. Biol.* **50**, 95–104 (2016).
- Gómez-Schiavon, M. & El-Samad, H. CoRa-A general approach for quantifying biological feedback control. *Proc. Natl. Acad. Sci. U. S. A.* **119**, e2206825119 (2022).
- Lefkowitz, R. J. A brief history of G-protein coupled receptors (Nobel Lecture). *Angew. Chem. Int. Ed. Engl.* **52**, 6366–6378 (2013).
- Christopoulos, A. & El-Fakahany, E. E. Qualitative and quantitative assessment of relative agonist efficacy. *Biochem. Pharmacol.* **58**, 735–748 (1999).
- Kenakin, T. P. Biased signalling and allosteric machines: New vistas and challenges for drug discovery. *Br. J. Pharmacol.* **165**, 1659–1669 (2012).
- Keov, P. *et al.* Molecular mechanisms of bitopic ligand engagement with the M1 muscarinic acetylcholine receptor. *J. Biol. Chem.* **289**, 23817–23837 (2014).
- Luttrell, L. M., Maudsley, S. & Bohn, L. M. Fulfilling the promise of ‘biased’ g protein-coupled receptor agonism. *Mol. Pharmacol.* **88**, 579–588 (2015).
- Stott, L. A., Hall, D. A. & Holliday, N. D. Unravelling intrinsic efficacy and ligand bias at G protein coupled receptors: A practical guide to assessing functional data. *Biochem. Pharmacol.* **101**, 1–12 (2016).
- Burgueño, J. *et al.* A complementary scale of biased agonism for agonists with differing maximal responses. *Sci. Rep.* **7**, 15389 (2017).
- Kenakin, T. A scale of agonism and allosteric modulation for assessment of selectivity, bias, and receptor mutation. *Mol. Pharmacol.* **92**, 414–424 (2017).
- Ehlert, F. J., Griffin, M. T., Sawyer, G. W. & Bailon, R. A simple method for estimation of agonist activity at receptor subtypes: Comparison of native and cloned M3 muscarinic receptors in guinea pig ileum and transfected cells. *J. Pharmacol. Exp. Ther.* **289**, 981–992 (1999).
- Griffin, M. T., Figueroa, K. W., Liller, S. & Ehlert, F. J. Estimation of agonist activity at G protein-coupled receptors: Analysis of M2 muscarinic receptor signaling through Gi/o, Gs, and G15. *J. Pharmacol. Exp. Ther.* **321**, 1193–1207 (2007).
- Chabre, M., Deterre, P. & Antonny, B. The apparent cooperativity of some GPCRs does not necessarily imply dimerization. *Trends Pharmacol. Sci.* **30**, 182–187 (2009).
- Park, P. S. H. & Wells, J. W. Oligomeric potential of the M2 muscarinic cholinergic receptor. *J. Neurochem.* **90**, 537–548 (2004).

39. Hu, J. *et al.* Structural aspects of M₃ muscarinic acetylcholine receptor dimer formation and activation. *FASEB J.* **26**, 604–616 (2012).
40. Redka, D. S. *et al.* Coupling of G proteins to reconstituted monomers and tetramers of the M₂ muscarinic receptor. *J. Biol. Chem.* **289**, 24347–24365 (2014).
41. Liste, M. J. V. *et al.* The molecular basis of oligomeric organization of the human M₃ muscarinic acetylcholine receptor. *Mol. Pharmacol.* **87**, 936–953 (2015).
42. Anderson, D. *et al.* Rapid generation of recombinant baculovirus and expression of foreign genes using the BAC-to-BAC Baculovirus expression system. *Focus Madison.* **17**, 53–58 (1995).
43. Randáková, A. *et al.* Agonist-specific conformations of the M₂ muscarinic acetylcholine receptor assessed by molecular dynamics. *J. Chem. Inf. Model.* **60**, 2325–2338 (2020).

Acknowledgements

This research was funded by the Czech Academy of Sciences institutional support [RVO:67985823], the Grant Agency of the Czech Republic grant [23-04670S] and the project National Institute for Neurological Research (Programme EXCELES, ID Project No. LX22NPO5107)—Funded by the European Union—Next Generation EU.

Author contributions

A.R. and D.N. designed, conducted experiments and analysed experimental data. J.J. derived equations for theoretical models and wrote Python code for model data analysis. All authors contributed to writing the manuscript, and read and approved the final version of the manuscript.

Competing interests

The authors declare no competing interests.

Additional information

Supplementary Information The online version contains supplementary material available at <https://doi.org/10.1038/s41598-023-45004-7>.

Correspondence and requests for materials should be addressed to J.J.

Reprints and permissions information is available at www.nature.com/reprints.

Publisher's note Springer Nature remains neutral with regard to jurisdictional claims in published maps and institutional affiliations.



Open Access This article is licensed under a Creative Commons Attribution 4.0 International License, which permits use, sharing, adaptation, distribution and reproduction in any medium or format, as long as you give appropriate credit to the original author(s) and the source, provide a link to the Creative Commons licence, and indicate if changes were made. The images or other third party material in this article are included in the article's Creative Commons licence, unless indicated otherwise in a credit line to the material. If material is not included in the article's Creative Commons licence and your intended use is not permitted by statutory regulation or exceeds the permitted use, you will need to obtain permission directly from the copyright holder. To view a copy of this licence, visit <http://creativecommons.org/licenses/by/4.0/>.

© The Author(s) 2023